Integrated Polyaniline-coated CF_x Cathode Materials with Enhanced Electrochemical Capabilities for Li/CF_x Primary Battery

Lei Li, Ling Zhu, Yong Pan[*]*, Weixin Lei*[*]*, Zengsheng Ma, Zhenzhen Li, Juanjuan Cheng, Jie Zhou*

Hunan Provincial Key Laboratory of Thin Film Materials and Devices, Xiangtan University, Xiangtan, Hunan 411105 China
[*]E-mail: ypan@xtu.edu.cn, wxlei@xtu.edu.cn

A core/shell structure CF_x (x = 1)/polyaniline integral composites are synthesized via an in situ chemical oxidative polymerization method at 0 ℃. The effects of the amount of aniline monomers (CF_x powers : aniline monomers = 4:1, 2:1, 4:3 in a weight ratio marked CF_x4:1, CF_x2:1, CF_x4:3 separately) are studied. The polyaniline is evenly coated on the surface of graphite fluoride and the appropriate thickness of polyaniline layer is about 160~180 nm. Synthetic materials discharge rate can reach up to 8 C, which is much higher than most of the currently available CF_x cathodes and the pristine CF_x. CF_x2:1 and CF_x4:3 discharge capacity still keep more than 700 mAh g^{-1} at 6 C and the power density can reach up to more than 10000 W Kg^{-1} at 8 C. All these can be attributed to the conductive polyaniline coating, which provides the exterior connectivity between particles for facile electron conduction, resulting in high-rate performance, high discharge capacity, high discharge voltage and high power density.

1. INTRODUCTION

In nowadays society, the battery has become an essential part of our life. Of cause, science research mainly focused on the secondary battery. Whereas high rate, high power density, high capacity primary battery is indispensable in military, aerospace and medical application. As one category of battery systems, primary batteries include alkaline zinc-manganese dioxide dry cell, zinc-mercury battery and lithium battery. Particularly, lithium battery usually contains Li/$SOCl_2$, Li/MnO_2 and Li/graphite fluoride (CF_x) primary batteries. Specially, compared to all these primary lithium

batteries, the theoretical specific capacity of Li/CF_x cell is much higher than the other cells, reaching up to 865 mAh g^{-1} when x = 1. In consequence, since graphite fluorides were used as positive electrode in primary lithium batteries firstly by Watanabe [1], it got more and more widely attention. Graphite fluoride is usually prepared from chemical reaction of fluorine with graphite at high temperature and it has two forms [2]. One is $(CF)_n$ which has been first successfully synthesized by Ruff and Bretschneider at 420 ℃ [3],and the other is $(C_2F)_n$ which was known as dicarbon monofluoride synthesized by Later Kita et al. [4] between 350 ℃ and 400 ℃. According to the temperature, the value of x in the CF_x can vary between 0 and 1.3, which is an average value because the two kinds of graphite fluorides, (CF) and (C_2F), were synthesized in the process of reaction at the same time. The overall discharge reaction of a Li/CF_x cell can be expressed as "$CF_x + xLi \rightarrow C + xLiF$". Based on this reaction, It is easily to find that lithium just react with fluorine when the cell discharging. So the specific capacity of a CF_x cathode is associated with the content of fluorine, i.e., x value in the formula [5] and it can be expressed as Eq. (1) [6].

$$Q_{th} = \frac{xF}{3.6(12+19X)} \qquad (1)$$

When the x value is too low, it is not conducive to exhibit the advantage of high specific capacity of CF_x. Theoretically, a CF_x with x = 1 has a specific capacity of 865 mAh g^{-1} and it is obvious higher than CF_x with a low x. But if the value of x is too high, the electronic conductivity of CF_x reduced rapidly. This is because the formation of a large number of C-F covalent bonds, which make the electronic conductivity of graphite fluoride material poor. So the low electronic conductivity of graphite fluoride materials lead to the electrode polarization easily, the low discharge rate property, the far lower actual discharge voltage platform compared with the open circuit voltage, especially under the condition of high rate discharge. As a matter of course, these disadvantages limit the application of CF_x in the fields requiring power densities [7-8].

In general, there are the following several kinds of methods to solve these problems. One of the effective methods is preparing sub-fluorinated graphite. Yazami et al. [5-6] synthesized a series of sub-fluorinated carbon materials with lower content of fluorine (CF_x, with x < 1). The cells' maximum discharge rate reach up to 6 C and the power density is higher than 8000 W Kg^{-1}. Sub-fluorinated graphite was also successfully obtained using thermal treatment methods [9-10] because of the partial decomposition of CF_x during the carbon thermal treatment. However, this is at the cost of the cell's specific capacity. This approach doesn't make good use the characteristics of high specific capacity of CF_x. Adding some highly conductive additives to the paste [11-16] to increase the electrical conductivity is another way. Simple physical mixing can improve electrical conductivity to a certain extent, but CF_x and additives are not worked as a whole. Therefore the battery discharge rate can only achieve 1 C. Then surface coating by conductive materials has also been used to improve the performance[17-18]. Making a conductive carbon coating of the CF_x powder [19] or modifying the graphite fluorides surface by electrodeposition of a conductive polypyrrole [20] which enhance the electronic conductivity of CF_x particles. The maximum discharge rate reach to 5 C, 4 C respectively. But this method is complicated and process conditions are demanding. Besides the methods mentioned above, there are many other ways[21-22]. Reducing the particle size by mechanical milling [23] and designing different arrangement of CF_x and MnO_2 hybrid cathodes [24] were also considered to

improve the performance of CF_x. The highest discharge rate and power density they can achieved is 6 C and 5C, 6599 W Kg^{-1} respectively.

In this paper, a core/shell structure CF_x/polyaniline (PANI) integral composites for use as a high-performance cathode material was prepared by an in situ chemical oxidative polymerization method for the first time. Doping conductive polyaniline was used as a conductive layer in order to increase the electrical conductivity of CF_x and improve the wettability between CF_x and electrolyte. CF_x materials with different thickness of the PANI layer were synthesized and were also discussed in this study.

2. EXPERIMENTAL

2.1. Preparation of CF$_x$/Polyaniline Composites

The CF_x/polyaniline (CF_x/PANI) composites were synthesized by an in situ chemical oxidative polymerization method at the freezing temperature in a mixed solution. The specific process is as follows. Three copies of CF_x (1 g) powders (Shanghai CarFluor Chemicals Co., Ltd) were respectively placed into deionized water (10 mL) containing the OP-10 emulsifier (Tianjin Chemical Reagent Company) for mechanical stirring for 30 min and then magnetic stirred for 6 h, so that the CF_x powders could be homogeneously dispersed. Different amounts of aniline monomers (0.25 g 0.50 g 0.75 g)(Tianjin Chemical Reagent Company), which had been purified by distillation, were added into dilute hydrochloric acid solution (2 mol L^{-1}, 10 mL). Then, the three CF_x solutions and the aniline monomers solutions were put into three different three-necked flasks and the mixtures were stirred vigorously for 10 min (CF_x powers : aniline monomers = 4:1, 2:1, 4:3 in a weight ratio marked CF_x4:1, CF_x2:1, CF_x4:3 separately). Subsequently, a hydrochloric acid solution of ferric chloride ((AR, Yantai Chemical Reagent Company) $FeCl_3$:aniline monomers = 4:1 by weight, $FeCl_3$ was dissolved in 10 mL hydrochloric acid solution) as an oxidant was added dropwise to the above reactant mixture, and the mixture in each flask was stirred for 12 h at 0 ℃ in an inert atmosphere. After polymerization, the reaction product was filtered and washed repeatedly with deionized water and ethanol until the washing solution became neutral pH and transparent to remove the iron ions and the unreacted aniline monomers. Then the reaction product was dried in a vacuum oven at 60 ℃ for 24 h to get the pure CF_x/PANI composites.

2.2. Material Characterization

X-ray diffraction (XRD) measurements were made using a Rigaku D/Max-2400 X-ray diffractometer with Cu K_α radiation ($\lambda = 0.1542$ nm). The surface morphologies and microstructures of the pristine CF_x and CF_x-Polyaniline composites were characterized by scanning electron microscopy (SEM, Hitachi S-4800) and transmission electron microscopy (TEM, JEM-200).

2.3. Electrochemical Study

To prepare the working electrodes，the CF_x and CF_x/PANI composites cathode slurry were made using a mixture of active material, acetylene black, and polyvinylidene fluoride (PVDF) in a weight ratio of 70:20:10 binder in an N-methyl-2-pyrrolidinone (NMP) dispersant to form a homogeneous slurry. Then the slurry was compressed into a thin piece with coating machine. Next, the coated electrodes were dried in a vacuum oven at 60 ℃ for 12 h. Subsequently, the electrode was cut into disks of 14 mm diameter and compressed with the tablet press. The coin-type 2016 cells were assembled in an argon-filled glovebox to avoid contamination by moisture and oxygen. The electrolyte used was 1 M $LiPF_6$–EC : DMC (1:1 by weight) solution. Lithium metal was used as anode, and a microporous polypropylene film (Celgard 2400) was used as a separator.

All the electrochemical measurements were carried out at room temperature. Electrochemical discharge performance, under the potential window 3.0-1.5 V vs. Li/Li$^+$, was conducted using Battery Test System (Neware, Shenzhen, China). Electrochemical impedance spectroscopy (EIS) was measured by a CHI660D Electrochemical Workstation (Chenhua, Shanghai, China) in the frequency range from 0.1 Hz to 1000 kHz.
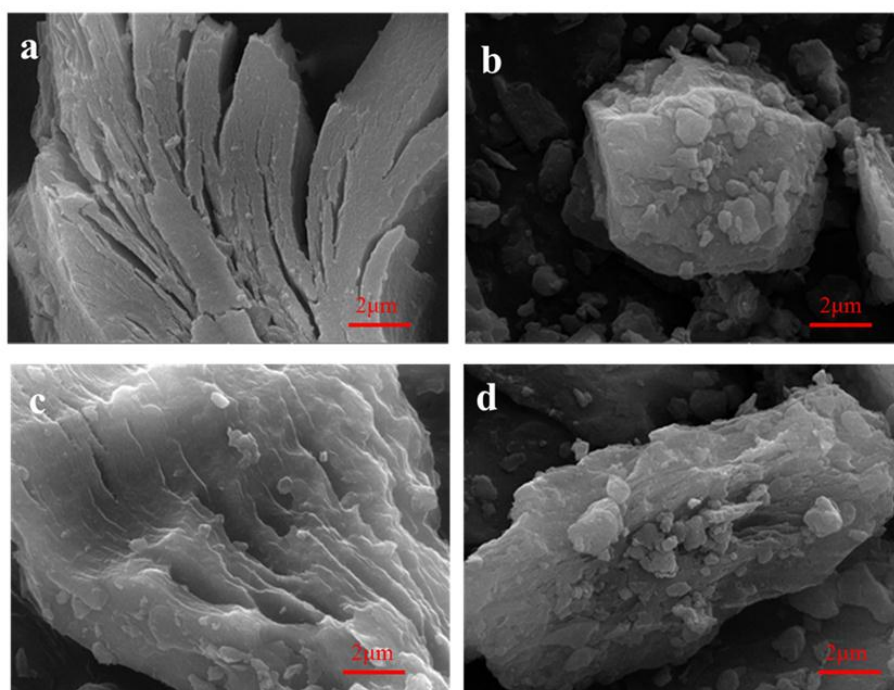
3. RESULTS AND DISCUSSION

Figure 1. SEM images of CF_x samples before and after coated PANI (a) Pristine CF_x; (b) CF_x4:1; (c) CF_x2:1; (d) CF_x4:3.

SEM images of both pristine CF_x and coated CF_x are shown in Fig.1. We can clearly find the morphology changed before and after coatings. The pristine CF_x surface is smoother and the texture is

clearer than the PANI coated CF_x powders, regardless of compared with CF_x4:1, CF_x2:1 or CF_x4:3. This can initially determine PANI has coated on the surface of CF_x. Meanwhile, from the EDS spectrum (not shown here) we detected the presence of nitrogen on the surface of the samples, which is the typical element of PANI compared with CF_x, indicating there is really a layer of PANI coated on the CF_x.
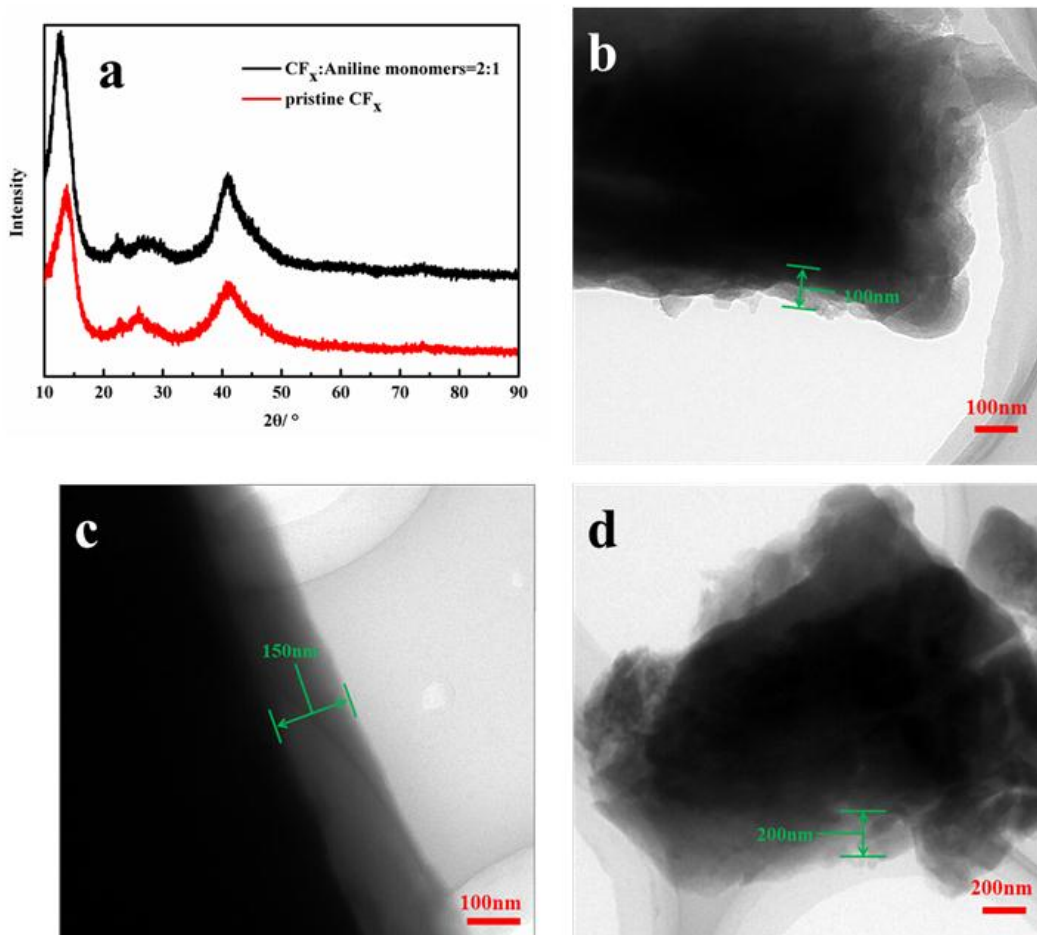

Figure 2. (a) XRD patterns of pristine CF_x and CF_x/PANI composite; TEM images of CF_x/PANI composites (b) CF_x4:1; (c) CF_x2:1; (d) CF_x4:3.

X-ray-diffraction (XRD) patterns of the pristine CF_x and the as-prepared CF_x/PANI composites (2:1) are presented in Fig. 2a. Only broad diffraction peak of CF_x were detected in both of the samples, demonstrating that the CF_x existed in a highly dispersed amorphous state, but do not find any diffraction peaks of PANI from the Fig. 2a. By the contrast analysis, the location and shape of the diffraction peaks don't change much after coating PANI. We conclude that the structure of CF_x remained original and no new phase was formed during the in situ polymerization oxidation process. What's more, the polymerized PANI layer is so thin that XRD undetectable.

To prove the existence of the core/shell structure of the CF_x/PANI composite, TEM images of CF_x4:1, CF_x2:1 and CF_x4:3 are presented in Fig. 2(b, c, d) respectively. From the TEM images of the CF_x/PANI composites, we can clearly find that all the three composites have a core/shell structure,

which shows the coating of PANI, where is translucent, on the surface of CF_x was successful. In addition, the thickness of the PANI coating layer increased with the increment of aniline monomers. It is about 100 nm of the CF_x4:1 composites. CF_x2:1 and CF_x4:3 composites are about 150 nm and 200 nm, respectively. According to the discharge curves in Fig. 3, the PANI coating thickness of about 160~180 nm is appropriate. The PANI coating acts as conducting layer, which plays conductive bridge role between the CF_x particles.
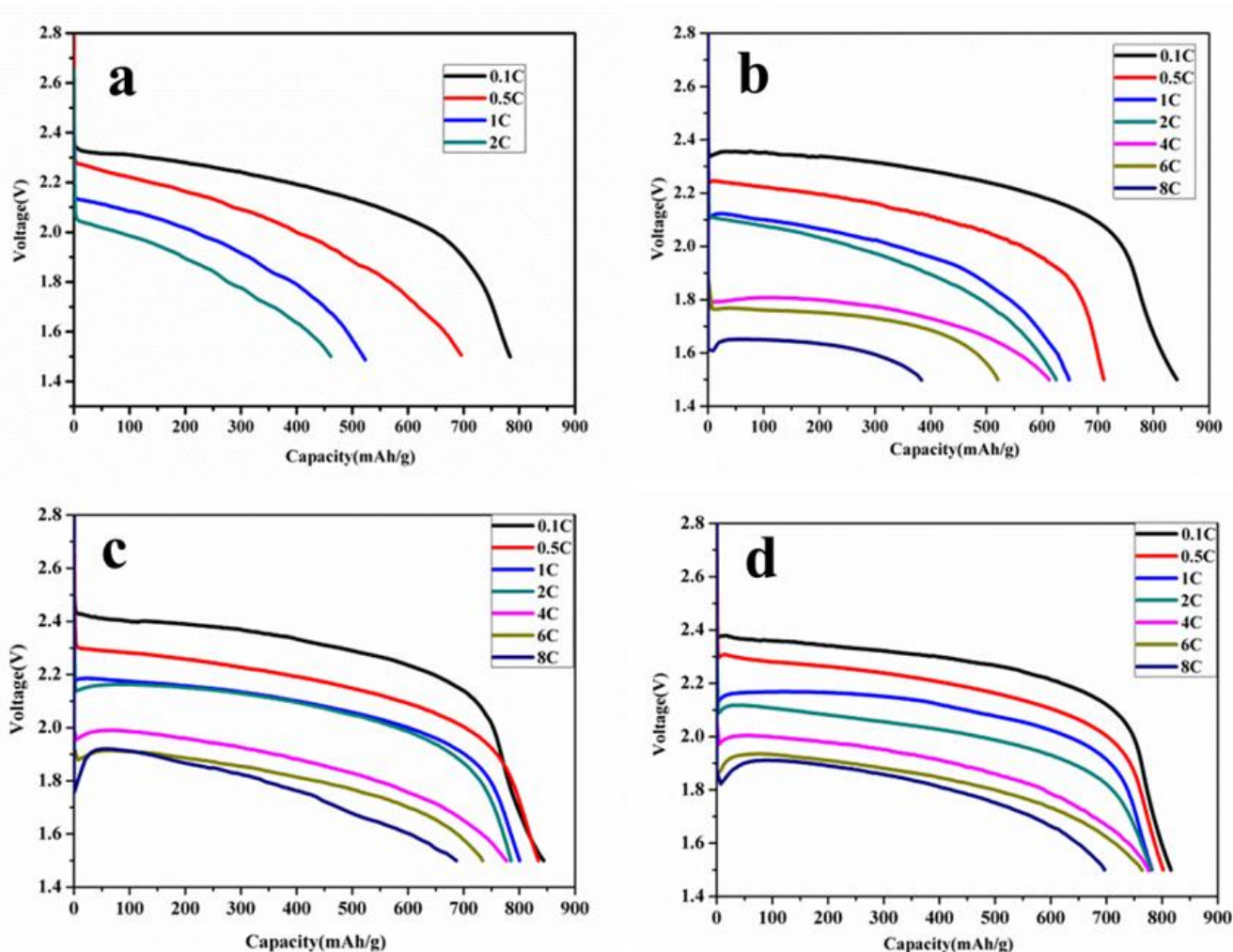

Figure 3. Galvanostatic discharge curves of (a) Pristine CF_x; (b) CF_x4:1; (c) CF_x2:1; and (d) CF_x4:3 obtained at different current densities.

The electrochemical performances of the pristine CF_x and CF_x/PANI composites materials have been studied in primary lithium battery for a potential cut-off of 1.5 V vs. Li^+/Li. The galvanostatic discharge curves of the samples are shown in Fig. 3, obtained at various discharging current densities. In the case of Li/CF_x cell (Fig. 3a), the average discharge potential is about 2.19 V at 0.1 C and the plateau is not steady, especially under the condition of high rate discharge. When discharge rate reached 0.5 C above, no obvious discharge plateau was found. Furthermore, the discharge voltage and the specific discharge capacity reduced quickly with the increase of discharge rate.

Compared with Li/CF$_x$ cell, all the three Li/CF$_x$/PANI cells showed much better discharge performance, whatever in any discharge platform, discharge specific capacity and discharge rate. Because PANI content is relatively few in the CF$_x$/PANI composite materials, the CF$_x$/PANI composite can be considered as active material. From discharge curves (Fig. 3(b, c, d)), the discharge voltage shows a higher plateau about 2.27 V (Fig. 3b), 2.32 V (Fig. 3c), 2.30 V (Fig. 3d) at 0.1 C, respectively, and they are much higher than Li/CF$_x$ cathode at other discharge rates. In addition, an obvious increase in specific discharge capacity is showed for the PANI-coated samples compared to the uncoated sample. It is about 842 mAh g^{-1}, 843 mAh g^{-1}, 815 mAh g^{-1} at 0.1 C respectively, which gets close to the theoretical specific capacity (865 mAh g^{-1}). The capacity of CF$_x$4:3 is lower than the other two samples because the PANI coating is so thick that the content of CF$_x$ is relatively reduced in composite materials, i.e. fluorine decreased, and parts of CF$_x$ can't participate in the reaction. Moreover, in terms of discharge rate, it can only get to 2 C of pristine CF$_x$, while an obvious increase in discharge rate is observed in the samples the CF$_x$4:1, CF$_x$2:1, CF$_x$4:3. They can reach up to 8 C, which is much higher than most of the currently available CF$_x$ cathodes. For example, the highest discharge rate of PPy-CF$_x$ composite material synthesized by the electrodeposition [20] is 4 C and the specific discharge capacity is only 70 mAh/g at 4 C. It may be caused by the following reasons. First of all, polyaniline and polypyrrole have different degrees of influence on the CF$_x$ material electrochemical performance. Coating layer thickness difference, which affect the charge transfer efficiency of the material, is another important cause of the electrochemical properties of CF$_x$ composite material. Then from the SEM and TEM images, CF$_x$/PANI integrity is very good. All this maybe lead to PPy-CF$_x$ composite material discharge rate can only reach 4 C. Currently reported the highest Li-CF$_x$ battery discharge rate can reach 6 C and the specific discharge capacity is more than 400 mAh/g at 6 C [5]. This is because they used fluorinated carbon nanofibers as electrode material and carbon nanofibers itself has good electrical conductivity. Then the carbon nanofibers they used didn't fully fluorinated so fluorinated carbon nanofibers keep a good electric conductivity. In this paper, the synthesized CF$_x$/PANI composite materials specific capacity can reach more than 700 mAh/g at 6 C, indicating that PANI layer has excellent electrical conductivity. With the increase of discharge rate, pristine CF$_x$ discharge voltage and discharge specific capacity reduced rapidly; nevertheless, the discharge voltage and discharge specific capacity of the CF$_x$/PANI composites reduce slowly from 0.1 C to 8 C. The voltage of all cells shows a current-related delay in the beginning of discharge at high discharge rates, because the resistance of ion transport in the electrolyte is predominant to control the discharge profiles. When the ions diffusion achieve balance, the voltage recovers to the normal voltage. This also suggests the PANI-coating has good enough electron transfer ability to meet the demand of high rate discharge in the case of CF$_x$/PANI composites.

Meanwhile, the effects of the proportion of CF$_x$ and PANI on the discharge performance of Li/CF$_x$ battery are also investigated. From Fig. 3(c, d), we can clearly see the discharge voltage steadily decreased but the discharge specific capacities only have a very small decrease, which keep more than 730 mAh g^{-1} at 6 C, indicating most of the CF$_x$ react with lithium in the process of discharge. But CF$_x$4:1 sample (Fig. 3b) can't catch up with the other two samples, because the PANI layer coated on the surface of the CF$_x$ is a little thin, leading electrical conductivity is not very well.
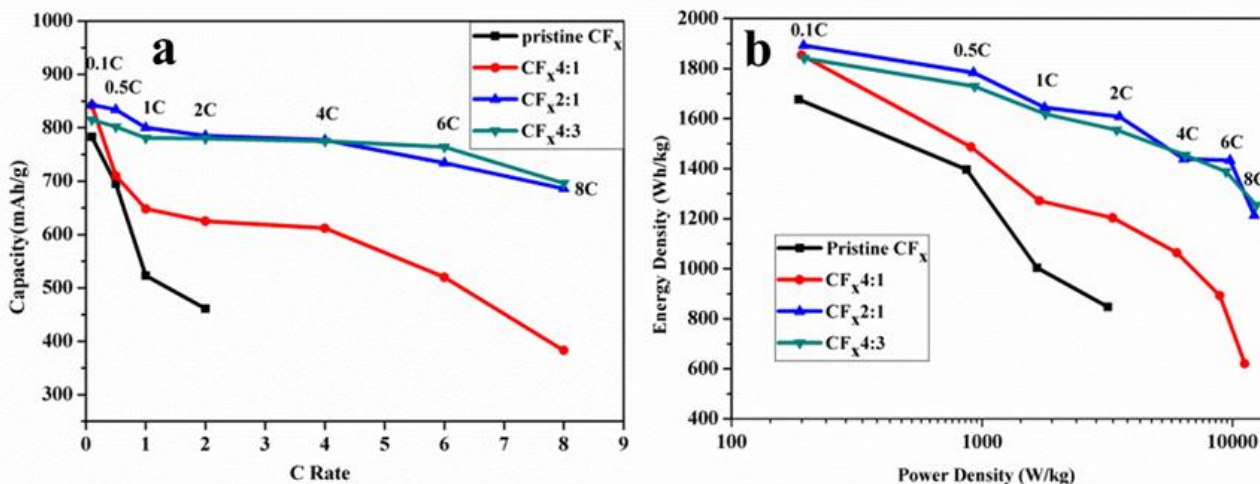
Figure 4. Comparison of (a) specific capacities of all the four cells vs. discharge current rate; (b) Energy density vs. power density (Ragone plot).

Fig. 4a is specific capacities of all the four cells vs. discharge current rate. It intuitively reflects $CF_x2:1$, $CF_x4:3$ discharge specific capacities are better than $CF_x4:1$. The specific capacities of $CF_x2:1$ and $CF_x4:3$ are almost similar to each other. The reason of discharge rate and discharge specific capacities improvement is attribute to the fact that the conductive PANI layer increase the contact between the particles thereby improving the facile electrical contact between the particles.

Fig. 4b shows the variation of the energy density versus power density (Ragone plot) of all the four samples studied. It is clearly observed that $CF_x2:1$ exhibit the best performance below 4 C rate and the pristine CF_x sample performance can not to be compared with other samples. In the case of high rate, all the three CF_x/PANI composites power density can reach up to more than 10000 W Kg^{-1} (at 8 C discharge rate), whereas only 3179 W Kg^{-1} was obtained with pristine CF_x (at 2 C discharge rate). The result turned out that the PANI coating layer has a positive influence on electrochemical performance.

The performance (rate capability, discharge specific capacities, discharge potential) improvement of CF_x is illustrated from the resistance by the electrochemical impedance spectroscopy (EIS) in Fig. 5.

The impedance spectroscopy for all of four cells were composed of a depressed semicircle in the high-frequency domain and followed by a slopping straight line in the low-frequency region. The depressed semicircle in the high frequency region corresponds to the cell reaction resistance (R_{cr}), which is the synergetic effects of the contact resistance between particles, product shell resistance and charge-transfer resistance of the electrolyte-electrode interface[25-26]. As shown in Fig. 5, the cell R_{cr} values decreased dramatically after coating, indicating an improved conductivity of the PANI-coated electrode. The pristine CF_x has the highest cell reaction resistance, while the resistance value of $CF_x4:1$ is about 130 Ω. However, the resistance values of $CF_x2:1$ and $CF_x4:3$ are both about 80 Ω. The conductivity of the composites does not increase obviously with the improvement of the thickness of the conductive PANI layer. Maybe this is because the synthesized PANI layer conductivity is limited.

This also explain why the specific capacities of CF_x2:1 and CF_x4:3 are almost similar to each other in Fig. 3(c, d).
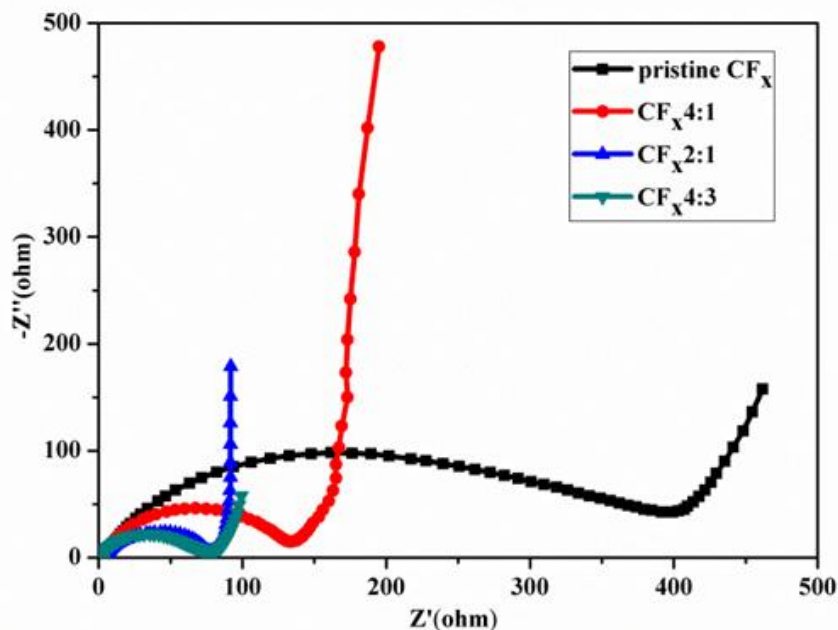

Figure 5. EIS patterns of pristine CF_x and CF_x/PANI composites; the EIS measurements were performed in the frequency range of 1 MHz to 0.1 Hz with an AC voltage amplitude of 5 mV at the open-circuit voltage.

4. CONCLUSIONS

In summary, CF_x/PANI integral composites with a core/shell structure can be synthesized by an in situ chemical oxidative polymerization method. None modification of the basic structure is observed by XRD after the PANI coated on CF_x. There is an outstanding electrochemical performance after coating: the discharge specific capacity get close to the theoretical specific capacity at 0.1 C; the maximum discharge rate for pristine CF_x is 2 C, whereas higher discharge rates up to 8 C can be used for CF_x/PANI integral composites; the power density can reach up to more than 10000 W Kg^{-1} under the condition of high discharge rate; the resistance values of CF_x/PANI integral composites cathodes decrease dramatically compared with the pristine CF_x cathode.

References

1.   N. Watanabe, M. Fukuda, Primary cell for electric batteries. *US, US3536532.* (1970).

2. N. Watanabe, T. Nakajima, H. Touhara (Eds.), *Graphite Fluorides, Elsevier, Amsterdam,* 1988, pp. 23-89.
3. O. Ruff, O. Bretschneider, *Zeitschrift für anorganische und allgemeine Chemie* 217 (1) (1934) 1-18.
4. Y. Kita, N. Watanabe, Y. Fujii, *J. Am. Chem. Soc. 101* (14)(1979) 3832-3841.
5. R. Yazami, A. Hamwi, K. Guérin, Y. Ozawa, M. Dubois, J. Giraudet, F. Masin, *Electrochem. Commun.* 9 (7) (2007) 1850-1855.
6. P. Lam, R. Yazami, *J. Power Sources* 153 (2) (2006) 354-359.
7. S. S. Zhang, D. Foster, J. Wolfenstine, J. Read, *J. Power Sources* 187 (1) (2009) 233-237.
8. N. Watanabe, R. Hagiwara, T. Nakajima, H. Touhara, K. Ueno, *Electrochim. Acta* 27 (11) (1982) 1615-1619.
9. S. S. Zhang, D. Foster, J. Read, *J. Power Sources* 188 (2) (2009) 601-605.
10. S. S. Zhang, D. Foster, J. Read, *J. Power Sources* 191 (2) (2009) 648-652.
11. Y. Li, Y. Chen, W. Feng, F. Ding, X. Liu, *J. Power Sources* 196 (4) (2011) 2246-2250.
12. P. Krehl, S. Davis, R. Rubin, H. Gan, E. Takeuchi , EP 1816695 A1, (2007).
13. P. Meduri, H. Chen, X. Chen, J. Xiao, M. E. Gross, T. J. Carlson, J.-G. Zhang, Z. D. Deng, *Electrochem. Commun.* 13 (12) (2011) 1344-1348.
14. K. Guérin, R. Yazami, A. Hamwi, *Electrochemical & Solid State Letters* 7 (6) (2004).
15. M. Nagata, J. Yi, H. Tsukamoto, *Ecs Transactions* 33 (39) (2011).
16. P. J. Sideris, R. Yew, I. Nieves, K. Chen, G. Jain, C. L. Schmidt, S. G. Greenbaum, *J. Power Sources* 254 (2014) 293-297.
17. W. Yang, D. Yang, S. Cai, Z. Yi, W. Wen, W. Ke, F. Yi, J. Xie, *J. Power Sources* 255 (255) (2014) 37-42.
18. L. Zhu, Y. Pan, L. Li, J. Zhou, W. X. Lei, J. H. Deng, Z. S. Ma, *Int. J. Electrochem. Sci.* 11 (2016),14-22.
19. Q. Zhang, S. D'Astorg, P. Xiao, X. Zhang, L. Lu, *J. Power Sources* 195 (9) (2010) 2914-2917.
20. H. Groult, C. Julien, A. Bahloul, S. Leclerc, E. Briot, A. Mauger, *Electrochem. Commun.* 13 (10) (2011) 1074-1076.
21. E. Rangasamy, J. Li, G. Sahu, N. Dudney, C. Liang, *J. Am. Chem. Soc.* 136 (19) (2014) 6874-7.
22. R. Jayasinghe, A. K. Thapa, R. R. Dharmasena, Q. N. Tu, B. K. Pradhan, H. S. Paudel, J. B. Jasinski, A. Sherehiy, M. Yoshio, G. U. Sumanasekera, *J. Power Sources* 253 (5) (2014) 404–411.
23. M. A. Reddy, B. Breitung, M. Fichtner, *ACS Appl. Mater. Interfaces* 5 (21) (2013) 11207-11211.
24. Y. Li, W. Feng, *J. Power Sources* 274 (2015) 1292-1299.
25. C. Barchasz, J.-C. Leprêtre, F. Alloin, S. Patoux, *J. Power Sources* 199 (2012) 322-330.
26. Y.-J. Choi, Y.-D. Chung, C.-Y. Baek, K.-W. Kim, H.-J. Ahn, J.-H. Ahn, *J. Power Sources* 184 (2) (2008) 548-552.